Ecological Indicators 122 (2021) 107325

Contents lists available at ScienceDirect

Ecological Indicators

journal homepage: www.elsevier.com/locate/ecolind

Assessing vegetation restoration potential under different land uses and climatic classes in northeast Iran

Ahmad Emamian [a], Alireza Rashki [a,*], Dimitris G. Kaskaoutis [b,c], Ali Gholami [a], Christian Opp [d], Nick Middleton [e]

[a] Faculty of Natural Resources and Environment, Ferdowsi University of Mashhad, Mashhad, Iran
[b] Institute for Environmental Research and Sustainable Development, National Observatory of Athens, Greece
[c] Environmental Chemical Processes Laboratory, Department of Chemistry, University of Crete, 71003 Crete, Greece
[d] Faculty of Geography, University of Marburg, Marburg, Germany
[e] St Anne's College, University of Oxford, UK

ARTICLE INFO

Keywords:
Vegetation trend
Growing Season NDVI
de Martonne index
Terrain Niche Index
Environmental restoration
Northeast Iran

ABSTRACT

This study examines the trends in vegetation cover using the Growing Season NDVI (GSN) time series in moderate spatial resolution (250 m) over Khorasan Razavi province, in northeast Iran, during the period 2004–2015. The province is largely desert, with extra-arid, arid, and semi-arid de Martonne climate zones dominating, while rangelands, shrublands and deserts cover most areas, making it an ideal territory for monitoring vegetation trends and implement future restoration projects. Most parts of the province and land-cover classes show no trends in vegetation cover, but large decreasing trends occur in areas covered by sand dunes, previously reforested lands and clay pit areas. Trends in various land-cover types are also examined as functions of the climatic class and the Terrain Niche index (TNI), which is characteristic of the topography, revealing large decreasing trends in the extra-arid climatic zone. In addition, most of the areas exhibit Hurst exponent values around 0.5, implying stochastic time series without any consistency and a likelihood of random vegetation and land cover changes in the future. This study also aims to determine likely future vegetation status and the most favourable areas for restoration projects through analysis of two indexes (Future Restoration Dispersal Index, FRDI and Future Uncertainty Dispersal Index, FUDI). The results show that reforestation, sand dunes and clay pits areas are the most favourable for implementing restoration projects, while the spatial distribution of the potential restoration classes reveals that the southern and northeastern parts of Khorasan Razavi province are the most favourable areas for establishing environmental restoration activities in order to avoid further degradation of ecosystems.

1. Introduction

Global ecosystems are constantly changing; this change may be a result of natural vegetation processes, such as sequencing and climatic variability or of human activities, such as land-use conversion, exploitation of natural resources and any kind of environmental degradation (Baude et al., 2019; Boiral et al., 2019). Vegetation plays an important role at the global scale in regulating the carbon-cycle balance, reducing greenhouse gases and mitigating climate change (Arora, 2002; Fang et al., 2004; Hu et al., 2010), while in desert and arid areas changes in vegetation cover are especially important for land degradation and susceptibility to wind erosion and dust emissions (Gholami et al., 2020a; Miri et al., 2021). Vegetation dynamics have also been recognized as one of the key factors in the change of terrestrial ecosystems over the globe (Suzuki et al., 2007; Fu et al., 2010; Kelly et al., 2011) and, therefore, systematic monitoring of vegetation changes is fundamental for future land management initiatives. Monitoring is the process of determining the change in the status of an object or phenomenon by observing it at different time scales and includes the use of multiple data to quantitatively examine the impacts of time on natural or anthropogenic phenomena (Hubbard and Hornsby, 2011; Yi et al., 2014). The cost of monitoring at executive levels is a prominent issue and, therefore, the use of new techniques for continuous environmental monitoring can be effective.

* Corresponding author.
E-mail address: a.rashki@um.ac.ir (A. Rashki).

https://doi.org/10.1016/j.ecolind.2020.107325
Received 22 March 2020; Received in revised form 18 December 2020; Accepted 25 December 2020
Available online 4 January 2021

The use of reasonably-accurate remote sensing data and techniques is one of the most appropriate methods (in terms of cost, manpower and time) to monitor vegetation changes from local to global scales (Shataee and Abdi, 2007). Since space technology has been developed in recent decades, satellite remote sensing is an outstanding method for observing vegetation dynamics and land use - land cover (LULC) changes (Kharol et al., 2013; Svoray et al., 2013; Vadrevu et al., 2015). The normalized difference vegetation index (NDVI) exhibits highly dynamic and variable measurements over land and it is widely used to monitor the health and production of vegetation over extensive areas and/or for desertification monitoring (Myneni et al., 1997; Tucker et al., 2001; Nemani, 2003; Ahmadi et al., 2019; Khusfi et al., 2020). In addition, NDVI and net primary productivity (NPP), along with other indices, have been commonly used to investigate vegetation changes as a part of monitoring or restoration projects (Zhang et al., 2012; Huang et al., 2013; Wu et al., 2013). Linear regression analysis has been a common method for examining the trends in NDVI time-series. The method has been questioned regarding its ability to capture non-linear characteristics of vegetation dynamics in arid environments (Shuang-cheng et al., 2008), but still continues to be popular in large-scale studies due to its simplicity (Fensholt et al., 2009).

Several studies have focused on past patterns in vegetation change (Hague, 2016; Wang et al., 2018; Kelly et al., 2020), while recent ones have undertaken predictions for future trends (Tong et al., 2016; Lei et al., 2016; Xiao et al., 2018; Lu et al., 2019; Sun et al., 2020). Climate change and its uncertain impact on vegetation patterns over the globe have led to uncertainty regarding the linkage between vegetation development and vegetation change. The mutual impact of climate change and vegetation poses another challenge to predictions about future trends (Braswell et al., 1997; Piao and Fang, 2003; Fabricante et al., 2009). There are two main approaches for assessing future vegetation development, (i) by analyzing historic vegetation data and their response to changes using statistical methods such auto-covariance, and (ii) by modeling the response of vegetation to changes under different scenarios. Bunting et al. (2016) used the SAVANNA model to analyze future patterns of vegetation cover in Kruger National Park under changing climate, and they pointed out that landscape resilience is not only impacted by the severity of the changing climate but also by the degree of management of such systems. Scientists tried to find a suitable method for predicting the trend of vegetation changes in the future. One of the introduced methods is the Hurst Index. Because of its novelty and to determine its problems and efficiency, this index have been evaluated in different areas under different circumstances.

Hurst (1951) introduced the H exponent in order to study the time-series of flow in the Nile River, while later on, Mandelbrot and Wallis (1969) theoretically refined it. Hurst Exponent (H) takes advantage of auto-covariance and has been commonly used to measure the stability of large data series in nature through the Rescaled Range Series Analysis (R/S). The rescaled range analysis is performed by dividing the range of the mean-adjusted cumulative deviate series (R) by the standard deviation of the time series (S). The robustness of (R/S) analysis has rendered it a prime measure for non-parametric studies in economics (Sánchez Granero et al., 2008) and its potential has also been recognized in several studies of vegetation dynamics (Yue-cong et al., 2008; Peng et al., 2012; Jiang et al., 2015; Tong et al., 2016, 2018).

Due to different topographic conditions, the large areas covered by diverse vegetation patterns and the effects of dust fallout and human interference, Khorasan Razavi province in northeast Iran constitutes an ideal area for studying vegetation changes and land restoration projects for different climatic classes and topographic characteristics. Several studies using various indices have examined the vegetation changes in this province (Azadbar et al., 2011; Bagherzadeh and Daneshvar, 2014; Shiravi and Sepehr, 2017; Ziyaee et al., 2018; Poorhashemi et al., 2019), but none of them has investigated the trend of vegetation changes for different topography and climate classes. Vaisi et al. (2016) studied the vegetation changes in Iran over a 17-year period (from 2000 to 2016) using two MODIS NDVI images with no spatial and temporal analysis, and they revealed an increase in vegetation degradation across the country. Concurrent analysis of the past vegetation changes and future predictions of the vegetation trends in Khorasan province is the main innovation of the current research, along with determination of areas suitable for future restoration projects.

This paper aims to investigate the vegetation trends in Khorasan Razavi province in northeast Iran over the period 2004–2015 and to analyze the vegetation dynamics for different land-cover types, climatic classes and Terrain Niche Index (TNI). The main objectives of the study are to characterize the spatial differentiation of vegetation trends and to identify favourable areas for implementation of vegetation restoration projects, while it is the first study examining these ecological issues in northeast Iran. Identifying areas for restoring vegetation is very important and constitutes a critical step in national efforts that contribute to land degradation neutrality, a key target of Sustainable Development Goal (SDG) 15, which urges countries to protect, restore and promote sustainable use of terrestrial ecosystems, sustainable management of forests, combat desertification, reverse land degradation and halt biodiversity loss (Gilbey et al., 2019). In the previous related research conducted by Tong et al. (2016), only natural factors were considered, while human management factors, which also play a major role, were ignored. Therefore, in a way to increase the accuracy of the vegetation predictions in future, land use classes and climate classification were added in the current research. This paper is also timely in a wider context, coming as it does on the eve of the UN Decade on Ecosystem Restoration (2021–2030).

2. Material and methods

2.1. Study area

Khorasan Razavi province covers an area of ~117,000 km^2, corresponding to approximately 7% of the total area of Iran, and is located between 56°19′ to 61°16′ East and 33° 52′ to 37° 42′ North (Fig. 1). It is the second most populated province of Iran, with a total population of about 6 million people, including the metropolis of Mashhad (second most populated city in Iran with about 2.5 million) and other smaller cities. The climate is characterized as arid and semi-arid with an annual-mean temperature of 17 °C and average annual precipitation ranging from 75 mm in the south to 390 mm in the north (Boroughani et al., 2020). The north part of the province is mostly covered by mountainous ranges, with fertile plains among them due to fair rainfall and availability of groundwater resources. In contrast, the southern part is mostly arid due to low rainfall and its proximity to the desert areas of southeast Iran and Afghanistan, with poor vegetation cover and limited agricultural lands. Rangeland is the dominant land type with favourable conditions for wind erosion. The mountain ranges are composed of sedimentary and volcanic rocks from the Mesozoic and Cenozoic periods, while the plain areas are mostly composed of Quaternary alluvium and extended playas (Ziyaee et al., 2018; Boroughani et al., 2020). The province is also downwind of dust flows originating from the Karakum desert in Turkmenistan and dried playas in the Aral basin during the summer season (Rashki et al., 2018; Ziyaee et al., 2018; Poorhashemi et al., 2019).

2.2. Dataset

2.2.1. NDVi

NDVI retrievals over the study province were taken from the Moderate Resolution Imaging Spectroradiometer (MODIS) product (MOD13Q1) during the period 2004–2015. MOD13Q1 is available within 16 days at a spatial resolution of 250 m (about 130 NDVI satellite images were used in regressions and analyses and a total of 83000Biliun pixels). Using the Maximum Value Composite (MVC) technique, the monthly maximum NDVI values were calculated at each pixel for each

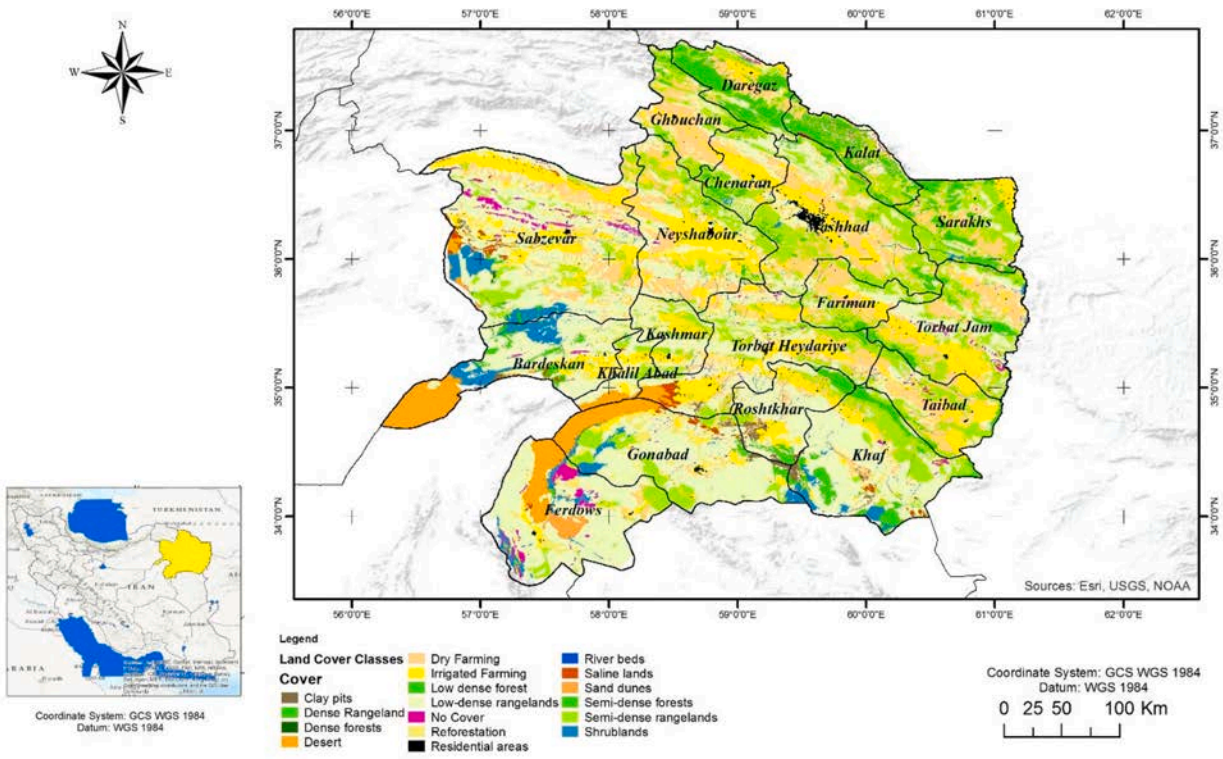

Fig. 1. Location of Khorasan Razavi province and spatial distribution of the land cover types.

year, which greatly reduce the atmospheric and scan/angle effects, cloud contamination and the effect of the high solar zenith angle (Holben, 1986). For minimizing the effects of random changes in vegetation, the Growing Season NDVI (GSN) was proposed. For calculating GSN, monthly NDVI values were averaged at each pixel during the growing season (March to September) for each year between 2004 and 2015 and these values were used in the whole analysis.

2.2.2. Digital elevation map (DEM)

Shuttle Radar Topography Mission (SRTM) Digital Elevation Map (DEM) images were downloaded from (https://earthexplorer.usgs.gov/) website at 90-meter spatial resolution, covering the whole Khorasan Razavi province. In order to collocate the size resolution of these cells with those of MODIS-NDVI, the resample technique and the nearest neighbor approaches were applied, and the size of each pixel was rescaled to 250 m (Tong et al., 2016). Using topographic maps of the region, basic maps of slope and elevation were produced.

2.2.3. Land use and land cover (LULC)

The digitized land cover map of Khorasan Razavi province was acquired from Forests, Range and Watershed Management Organization of Iran. These maps have been prepared for the whole Iranian territory with a scale of 1:250,000 since 2003. According to these maps, land is classified into 17 land-cover types as follows: no vegetation cover and rocky outcrops, saline lands, river beds, shrubland, sand dunes, dense forest, low-dense forests, semi-dense forests, reforestation, clay pits, irrigated farming, dry farming, desert, low-dense rangelands, dense rangelands, semi-dense rangelands and residential areas (Fig. 1).

2.3. Linear regression of NDVI trends

The linear regression of the averaged NDVI between March to September (Growing Season NDVI; -GSN) was performed over the whole province during the study period (2004–2015), in order to investigate the spatial pattern and intensity of the vegetation changes. The GSN was estimated as the average NDVI value at each pixel from March to September, which is considered as the growing season in this area. Positive slopes over the years indicate an increasing trend in vegetation, which could be attributed to climatic factors or the implementation of restoration projects, while negative values imply a decline in vegetation cover as a result of anthropogenic (exploitation, mining activities, abandoned cultivated lands, etc) and natural processes (desertification due to increased drought). To determine the significance of the GSN trends, the T-test was applied and p values were calculated for each pixel. A p value greater than 0.05 implies that the change is statistically meaningless at the 95% confidence level (C.L.) and the pixel falls into the category of "stable pixel" (unchanged). However, if p is<0.05, the change is statistically significant at the 95% C.L. Using this criterion, the examined area was divided into 3 classes corresponding to stable ($p \geq 0.05$), increasing (slope ≥ 0 and $p < 0.05$) and decreasing (slope ≤ 0 and $p < 0.05$) GSN.

2.4. Terrain Niche index (TNI)

The Terrain Niche Index is related to topographic conditions such as elevation and mountainous slope and is calculated based on the following formula (Tong et al., 2016).

$$TNI = log\left[\left(\frac{e}{E}+1\right)+\left(\frac{s}{S}+1\right)\right] \quad (1)$$

where:
e = pixel elevation from above mean sea level (amsl)
E = average sea-level elevation of the study area
s = topographic slope of the pixel
S = average topographic slope of the study area

The larger TNI values represent a higher elevation and/or steep slopes such as peaks and rocky hills in the studied pixel. On the other hand, the lower TNI corresponds to areas with smooth slopes and low altitudes, such as plains. The median values of the TNI represent areas with a high slope and low elevation, or a low slope and high elevation, or an area that has moderate conditions for both factors. The TNI map for Khorasan Razavi province can be seen in Suppl. Fig. 1.

2.5. Climatic classification

The de Martonne index (de Martonne, 1942) indicates the aridity conditions of an area and it is calculated by the Equation (2):

$$I = \frac{P}{10 + T} \tag{2}$$

where P is the annual rainfall (in mm) and T is the annual mean temperature (in Celsius). In our case, the P and T annual values were taken from 181 synoptic meteorological stations over the province during the period 1970 – 2005. The de Martonne index classification (Suppl. Fig. 2) was produced at spatial resolution of 250 m using the kriging regression method based on the data from the meteorological stations. In general, the province can be divided into 5 climatic classes: extra arid, arid, semi-arid, Mediterranean and semi-humid. Most areas are characterized by the "arid" climatic type, while a large part in the southwest is characterized as extra arid (Rahimi et al., 2013). Central-north areas are mostly semi-arid, while the Mediterranean-type and semi-humid areas are very limited, located at the top of the two highest mountainous ranges, which receive more rainfall and are snow-covered for several months.

2.6. Hurst exponent

The Hurst exponent (H) is based on automated covariance and is estimated through the "*Rescaled Range Series Analysis*." It quantitatively indicates the continuity or non-continuity of data series for natural phenomena in a specified time period (Hurst, 1951; Peng et al., 2012). For a time series of length N, the rescaled range analysis can be applied as follows (Lotfalinezhad and Maleki, 2020):

1. First, divide time series of length N to d new subseries $(Z_{im})$of length n.
2. For each subseries $(m = 1, 2, \cdots, d)$ calculate $(X_{im}) = (Z_{im})$ - (E_m) for $i = 1, 2, \cdots, n$. In this formula, $E_m$is the mean of subseries.
3. Then calculate the cumulative sum of the subseries as $Y_{im} = \sum_{j=1}^{i} X_{im}$ for $i = 1, 2, \cdots, n$.
4. After that the range $R_m$and standard deviation S_m of each subseries were used to calculate the rescaled range(R_m/S_m).
5. The mean rescaled ranges(R_m/S_m) were calculated for all subseries with length of n.
6. By assuming a power-law relationship between R/S and subseries length (n), we can obtain $(R/S) \approx cn^H$, and the H values could be simply obtained via regression on increasing samples using Equation (3):

$$\log\left(\frac{R}{S}\right)_n = \log c + H\log n \tag{3}$$

The Hurst exponent ranges between 0 and 1. H values around or equal to 0.5 indicate a stochastic time series without any consistency, suggesting randomness of the vegetation changes in the area and no relationship between environmental factors and vegetation changes in the future. If H ranges between 0.5 and 1, it indicates a "persistence-behavior" (auto-positive correlation), and as H approaches 1, more stability will be observed in the data. In contrast, H<0.5 represents "non-persistence behavior" (auto-negative correlation), while as H approaches 0, the anti-stability behavior in the data series will increase.

H index was applied in the GSN time series at the various pixels covering the whole Khorasan Razavi province. Based on the vegetation trends and H values, the study area was divided into six classes. If H is greater than 0.5 with a positive trend, the class is supposed to have a continuous increasing (Positive Development, PD), while if H is greater than 0.5 and the trend is negative, the class is considered as continuous decreasing (Negative Development, ND). In the case of H < 0.5 and a positive trend, vegetation is likely to stop increasing (Anti Positive Development, APD), whereas if H is<0.5 with a negative vegetation trend, the declining of vegetation will likely stop (Anti Negative Development, AND). Finally, if H greater than 0.5 and the trend is not significant, the pixel is categorized in the stable development class (SD) and if H < 0.5 is associated with a non-significant trend, the class is undetermined (UD) (see Suppl. Table 1).

2.7. Assessing restoration potential

To determine the future vegetation status in the area, two comprehensive indices were used. The Future Restoration Dispersal Index (FRDI) specifies which areas (classes) have more potential for a restoration project, while the Future Uncertainty Dispersal Index (FUDI) determines the rate of this uncertainty. These indices are calculated as follows (Tong et al., 2016):

$$FRDI_i = \frac{\left(\frac{e_{i1}+e_{i2}+e_{i3}}{a_i}\right)}{\left(\frac{E_1+E_2+E_3}{A}\right)} \tag{4}$$

$$FUDI_i = \frac{\left(\frac{e_{i4}+e_{i5}+e_{i6}}{a_i}\right)}{\left(\frac{E_4+E_5+E_6}{A}\right)} \tag{5}$$

where e_{ij} correspond to $j = 1$(PD), 2(SD), 3(ND), 4(UD), 5(APD), 6(AND) taken from the categories of the H exponent (section 2.6) and $i =$ TNI interval, de Martonne class and the land-cover classes, while $a_i$corresponds to the area of each class and A is the total study area.

$FRDI_i$and $FUDI_i$ indices are dimensionless and standardized. If $FRDI_i$ is greater than 1, it is supposed that the studied class exhibits more favourable conditions for restoration compared to other classes. In other words, the higher the $FRDI_i$, the greater potential for restoration. For larger $FUDI_i$ the prediction of the changes in that class is more uncertain; therefore, the lower the*FUDI*, the more reliable conditions for restoration. These combined results are included in Suppl. Table 2. Therefore, Class 4 exhibits the most favourable conditions in terms of restoration prospects and Class A has the least uncertainty (most definite), suggesting that A4 is the most favourable class with the lowest degree of uncertainty and F1 is the most unfavourable class with the highest degree of uncertainty (Suppl. Table 2). After combining the two *FRDI* and *FUDI* indices, the studied classes of LULC, de Martonne and TNI were categorized based on the favourability of the factors for development of vegetation, as well as its uncertainties. Finally, a map of the restoration potential was constructed for the Khorasan Razavi province.

3. Results

3.1. Vegetation dynamics and trends

The spatially-averaged NDVI over Khorasan Razavi province during the growing season (March to September) of the study period (2004–2015), was found to be 0.17, ranging from 0.14 (in 2008) to 0.19 (in 2009). The decadal variability (Suppl. Fig. 3) does not display a statistically-significant (95% C.L.) trend, although presenting a slight decreasing tendency. The spatial distribution clearly shows that GSN is heterogeneously scattered throughout the study area, with a general decreasing gradient from the northern to southern parts of the province (Fig. 2). The high-elevation areas such as the Hezar Masjed and Binalood mountains exhibited GSN values usually above 0.5, due to higher precipitation in the mountains. The vegetation in these mountainous areas is scattered trees and semi-dense forests or rangelands. In the northern parts of the province, there is a significant increase in vegetation cover after seasonal rainfall due to sufficient seed banks. However, this increase lasts for about 40 days, mostly reflecting the growth of annual grasses. The lowest GSN values are detected in the south and southwest

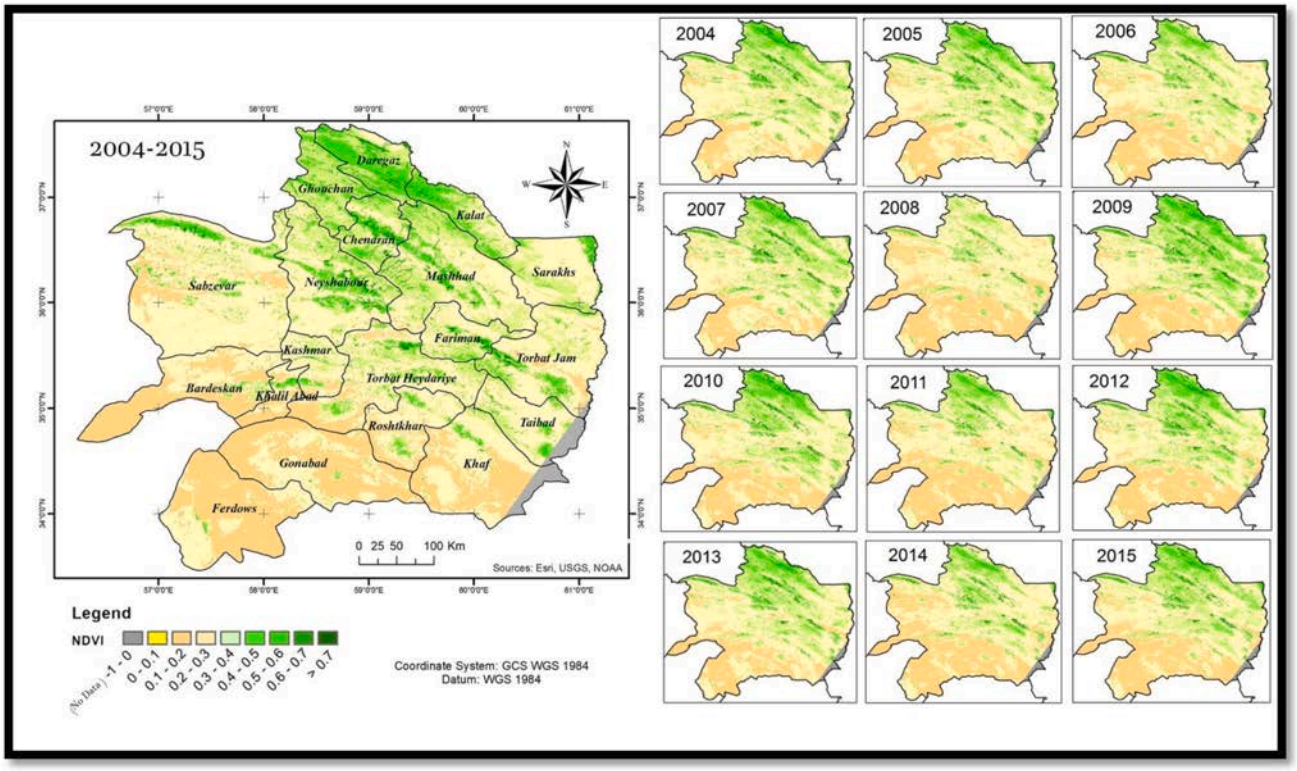

Fig. 2. Growing season NDVI (March to September) maps in the Khorasan Razavi province from 2004 to 2015. To the left, the mean map for the entire study period is shown. Grey area is not regularly covered by the satellite overpass and was excluded from the analysis.

parts of the province, which are mostly covered by sand dunes, shrublands and low-dense rangelands (Fig. 1) and are characterized by extra-arid climate (Suppl. Fig. 3). The total area and the spatial–temporal-averaged GSN values for each vegetation type are summarized in Table 1. The low-dense and semi-dense rangelands are the vegetation types with the largest coverage, followed by dry farming, while the semi-dense and dense forests cover the lowest areas in Khorasan Razavi. In addition, saline lands displayed the lowest GSN (0.07), followed by deserts and clay pits, while the highest GSN values were shown for irrigated farming (0.292) and dense forests (0.261) (Table 1).

Using linear regression analysis, the spatially-averaged GSN values showed an overall slight decreasing trend during the study period but without any statistical significance ($p = 0.47$). Further analysis revealed that fifteen out of the seventeen LULC types presented mostly a declining trend during 2004 – 2015, while the desert areas and the semi-dense forests revealed mostly increasing vegetation cover (Table 1). Reforestation was found to exhibit the largest downward trend, being statistically significant at 95% confidence level ($p = 0.016$). Regarding the reforestation, much more pixels (38.1%) displayed a downward rather than upward (0.6%) trend, while a significant decrease mainly occurred in Gonabad county, located in the southern province. This decreasing trend in reforestation is likely attributed to the fact that previous restoration projects were generally not well supported for a long term and were practically abandoned after implementation. Unfortunately, this operation destroyed the current vegetation cover and made the soil and vegetation vulnerable to degradation. In addition, droughts have

Table 1
Total area, average growing season NDVI (March to September) (Mean from 2004 to 2015), Hurst values and trends in vegetation for each LULC type in Khorasan Razavi province from 2004 to 2015.

	Land cover	Area (ha)	GSN	Trend (%)			Hurst(H)
				Stable	Increasing	Decreasing	
1	**No vegetation cover lands and rocky outcrops**	137,427	0.113	87.0	2.6	10.5	0.466
2	**Saline lands**	73,437	0.07	82.5	3.0	14.6	0.499
3	**River beds**	34,299	0.114	85.4	2.0	12.5	0.454
4	**Shrublands**	415,569	0.112	79.2	1.2	19.6	0.467
5	**Sand dunes**	43,924	0.102	47.7	1.1	51.2	0.528
6	**Dense forests**	4080	0.261	99.3	0.1	0.6	0.426
7	**Low dense forest**	484,072	0.251	91.5	2.6	5.8	0.463
8	**Semi-dense forests**	29,477	0.214	93.4	0.9	5.7	0.45
9	**Reforestation**	203,378	0.114	61.3	0.6	38.1	0.506
10	**Clay pits**	72,599	0.092	67.8	1.3	30.9	0.506
11	**Irrigated Farming**	162,646	0.292	85.7	2.1	12.1	0.455
12	**Dry farming**	1,934,227	0.186	91.9	0.8	7.3	0.437
13	**Desert**	362,278	0.078	85.5	13.8	0.7	0.488
14	**Low density rangelands**	4,816,849	0.126	81.0	2.3	16.7	0.476
15	**Dense rangelands**	315,871	0.240	97.5	1.8	0.7	0.435
16	**Semi-dense rangelands**	2,231,149	0.173	90.1	3.5	6.5	0.454
17	**Residential areas**	57,692	0.210	76.7	8.1	15.2	0.486

had a greater impact on this degradation. In addition, statistically-significant decreasing trends were also found for the sand dunes, shrublands and clay pit lands (Table 1). Similarly, saline lands, shrublands and low-dense rangelands exhibited much larger decreasing-area fractions, while the dense forests exhibited the highest area with no trend among the land-cover types (99.3% of the pixels are characterized as stable), which implies good management and protection of the forested areas.

By applying the de Martonne climate classification (Suppl. Fig. 2) in order to investigate the influence of climate conditions on vegetation, the extra-arid regions show a minimum GSN of 0.096, while the Mediterranean-climate type and the humid regions (although very limited in space) indicated the maximum GSN values (Table 2). Examining the vegetation trends according to the climatic classes, the semi-arid class exhibited the most stable conditions, so that in 93.9% of this class, the vegetation had no significant change (Table 2). The GSN exhibited a decreasing trend in 23.6% of the extra-arid class (statistically-significant at the 95% C.L.), while the highest level of increasing GSN was shown in the semi-humid class (19.2%). In general, the arid climate types exhibited a large decreasing fraction of GSN, while the Mediterranean-type and semi-humid climates displayed mostly increasing trends.

Furthermore, the whole province was divided into seven TNI classes, in order to examine the changes in GSN as a function of topography (Table 3). TNI Class 1 (areas with combination of lowest slope and lowest altitude) exhibited a moderate GSN (0.207), likely attributed to the larger coverage of agricultural lands in this class. Class 2 exhibited the lowest GSN of 0.148, since it includes areas with relatively low elevation and low slope, which are mostly lied in the extra-arid and arid climate classifications (Suppl. Fig. 1). GSN progressively increases with increasing TNI until Class 7 (areas with combination of the high slope and/or highest altitude), reflecting an increasing tendency of vegetation cover with altitude, whereas a slight decrease occurs for Class 8 (Table 3). This decrease is likely attributed to very high elevation (mountain tops) and/or very steep mountainous slopes, which are unfavourable for vegetation growth. Concerning the vegetation trends as a function of TNI class, GSN decreased in 18.6% of the TNI Class 2, while the lowest decreasing area (0.6%) in vegetation, also associated with the highest increasing fraction (11%), was recorded in Class 7, indicating a GSN increase in the high-elevated areas.

The GSN trends at each pixel over the study area were grouped into four categories, according to the statistical significance of the increasing or decreasing trends (Fig. 3). The results display a spatial differentiation in the vegetation trends from 2004 to 2015, revealing a predominance of decreasing trends in the south and increasing ones in the central-north parts of the province, especially along the mountainous ranges (Fig. 3). However, areas with statistical significant trends in vegetation cover (GSN) were limited, since 12% of the province displayed decreasing and only 2.6% increasing trends. Apart from the natural causes, mismanagement of land and water resources through construction of storage dams, diversion channels, changing patterns of cultivation and LULC changes have exacerbated vegetation loss, creating land areas susceptible to wind erosion and vulnerable to dust-storm outbreaks (Mosavi Baygi and Ashraf, 2011; Gholami et al., 2020b).

3.2. Spatial distribution of the Hurst exponent

This section analyzes the vegetation trends in Khorasan Razavi province based on the Hurst Exponent values. Fig. 4 shows the spatial distribution of H, which presents a remarkable spatial variability, ranging from 0.07 to 0.69. The spatially-averaged annual mean value during 2004–2015 was found to be 0.46, indicating a relative instability of the trends in vegetation cover. H values above 0.5 were detected in 33.6% of the area, mostly in the southern parts of the province, indicating that the vegetation cover will continue its existing trends, which were found to be highly decreasing in the most of these areas (see Fig. 3). H values above 0.6 are also detected in some parts of the north Khorasan Razavi (Chenaran, Sarakhs and small parts of Quchan county) (Fig. 4), which were mostly associated with increasing GSN trends (Fig. 3). Thus, this increasing vegetation trend has great possibility to be continued in the future. In 7.7% of the province, the future changes in vegetation would be completely random. Areas with H index below 0.5 are spread throughout the province covering the 58.7% of its area, implying that the sign of the vegetation trend is likely to change.

On the other hand, the averaged H values were found to vary slightly among the different land-cover types (Table 1). Sand dunes exhibited the highest mean H value (0.528), followed by clay pits and reforestation, while the lowest mean H values were recorded for dense forests (0.426), dense rangelands (0.435) and dry farming (0.437), indicating rather random and uncertain changes in GSN in most of these land-cover types (Table 1). Studying the H values as a function of the climatic classes (Table 2), the results showed random and rather uncertain changes for all climatic classes, since the H values were close to 0.5, ranging slightly from the semi-humid class (0.525) to the semi-arid class (0.446). Similarly, the H values did not present large fluctuations between the various TNI classes (Table 3). TNI Class 1 indicated random vegetation trends in the future ($H = 0.503$), while all the other classes exhibited H values slightly below 0.5, meaning that the vegetation trend may change.

3.3. Perspectives for environmental restoration

Identification of areas appropriate for environmental restoration is very important for maximizing benefits in terms of cost and time and has been given greater emphasis as part of national efforts towards achieving land degradation neutrality (Kiani-Harchegani and Sadeghi, 2020). The best way to select an area for restoration projects is to monitor the behavior of vegetation in the past, and then identify those areas likely displaying the same trends in the future (Hanson et al., 2013; Burnett et al., 2019).

As explained in section 2.6, combining the spatial distributions of the trends in vegetation cover (Fig. 3) and the H exponent (Fig. 4), the whole province can be divided into six classes representing various environmental restoration scenarios (PD, ND, APD, AND, SD and UD) (Fig. 5). The analysis showed that in 25.7% of the province area, stable conditions dominated, including mostly the eastern and southern parts. In 2.3% of the study area, such as the southern hillsides of Binalood, GSN will likely increase steadily (PD), while in 0.4% of the province, it is more likely that the positive trend will reverse (APD). The vast areas of the southern part of the province are likely to continue their decreasing

Table 2
Total area, average growing season NDVI (March to September) (Mean from 2004 to 2015), Hurst values and trends in vegetation for the de Martonne classes in Khorasan Razavi province from 2004 to 2015.

Class	De Martonne Zone	Area (ha)	GSN	Trends (%)			Hurst(H)
				Stable	Increasing	Decreasing	
1	Extra Arid	2,400,540	0.096	72.92	3.44	23.64	0.495
2	Arid	5,990,993	0.153	84.29	1.30	14.4	0.462
3	Semi-Arid	28,912	0.229	93.92	3.69	2.39	0.525
4	Mediterranean	143,167	0.283	88.97	10.99	0.04	0.501
5	Semi Humid	4,279,191	0.258	80.73	19.17	0.1	0.446

Table 3
Total area, average growing season NDVI (March to September) (Mean from 2004 to 2015), Hurst values and trends in vegetation for the TNI classes in Khorasan Razavi province from 2004 to 2015.

Class	TNI	Area(ha)	GSN	Trends (%)			Hurst(H)
				Stable	Increasing	Decreasing	
1	0.07–0.2	121,670	0.207	92.7	4.4	2.9	0.503
2	0.2–0.4	5,370,252	0.148	79.1	2.3	18.6	0.477
3	0.4–0.6	3,551,313	0.159	87.1	0.8	12.1	0.447
4	0.6–0.8	1,672,884	0.186	93.6	1.9	4.5	0.440
5	0.8–1	1,100,795	0.210	93.1	4.9	2.1	0.461
6	1–1.2	726,074	0.233	90.8	8.2	0.9	0.475
7	1.2–1.4	296,377	0.246	88.4	11.0	0.6	0.483
8	1.4–1.97	3437	0.236	88.8	10.0	1.2	0.488

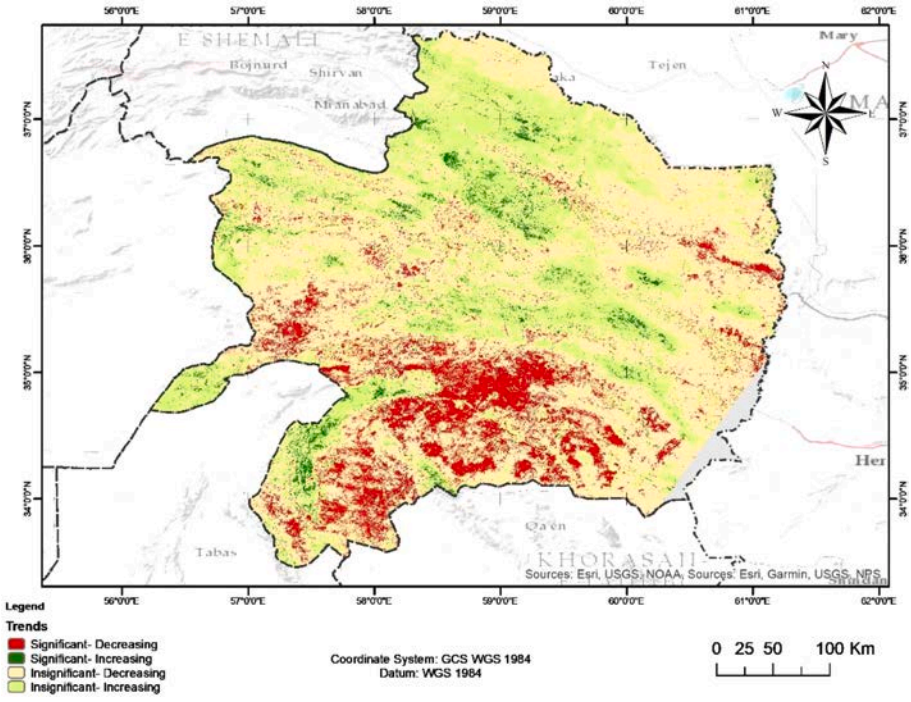

Fig. 3. Spatial distribution of the trends in vegetation cover in Khorasan Razavi province between 2004 and 2015. The significance of the trends corresponds to 95% confidence level.

tendency in vegetation, since about 9.4% of the study area will experience vegetation degradation (ND). On the contrary, the analysis showed that in 2.6% of the province area the current GSN reduction would disrupt, which implies that the vegetation cover will increase or have a stable condition (AND) in the future. Finally, the tendency of the uncertain vegetation development (UD class) covers the most part (56.6%) of the province (Fig. 5).

The analysis revealed that 79.4% of the dense forests and 77.4% of the dense rangelands did not indicate a specified trend, implying that changes in these land-cover types will not be stable, making it impossible to predict future changes using the current model (Table 4). Furthermore, in 73% of the dry farming class, the vegetation was also characterized as undetermined, which could be due to the unstable nature of this type of agriculture activity. The highest fractions of a land-cover type with stable conditions were recorded for saline lands (38.4%) and desert (34.6%). According to the analysis, it was predicted that the vegetation would present a continuous decreasing trend in 33% of reforestation areas, which shows that prior restoration projects have not been so successful. In addition, roughly the half of the sand-dunes will suffer from degradation in the future. Unlike sand dunes, only 0.2% of the dense-forests class will have a negative trend in vegetation. As mentioned above for the AND scenario, the pixels within this class are likely to show a different trend in the future (stable or increasing). The highest rate of change was predicted for the sand dunes (9.2% of the class area) followed by shrublands (6.4%), whereas the least fraction area of change was found for the dense rangelands (0.1%). APD is the reverse condition of AND, on which the current positive trend is expected to change to negative or stable. Desert exhibits by far the highest fraction of area for APD (3.4%) (Table 4).

For defining the restoration potential of the various LULC types (Suppl. Table 3), six conditions (A3, A4, B2, B3, C1 and D1) were observed in the study area. Seven LULC types including river beds, low-dense forest, semi-dense forest, irrigated farming, dry farming, dense rangeland and semi-dense rangeland were categorized as class C1, which means that they don't have a good potential for restoration and the restoration uncertainty is rather high. This may be likely attributed to the climate-change scenario in Iran and the Middle East with a decrease in precipitation pattern and increase in temperature (Mathew et al., 2002; Soltani and Gholipoor, 2006; Sharifikia, 2013; Zoljoodi and Didevarasl, 2013). Dense forest was labeled as D1, suggesting even higher uncertainty in comparison to C1 class. In contrast, reforestation, sand dunes, clay pits were tagged as A4 areas, suggesting that these classes are the most favourable for proposing restoration projects (Suppl. Table 3). The spatial distribution of the potential restoration classes in Khorasan Razavi province is shown in Fig. 6, where specific regions in the southern and western parts of the province (B3 to A4)

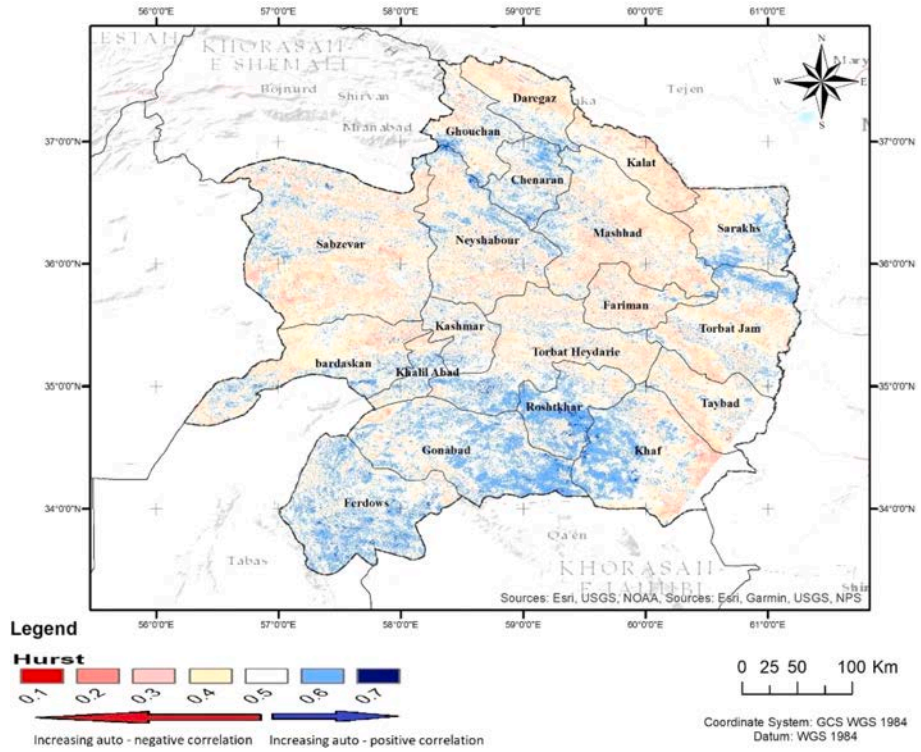

Fig. 4. Spatial distribution of the Hurst exponent in Khorasan Razavi province. Hurst exponent measures the stability of large data through the Rescaled Range Series Analysis (R/S).

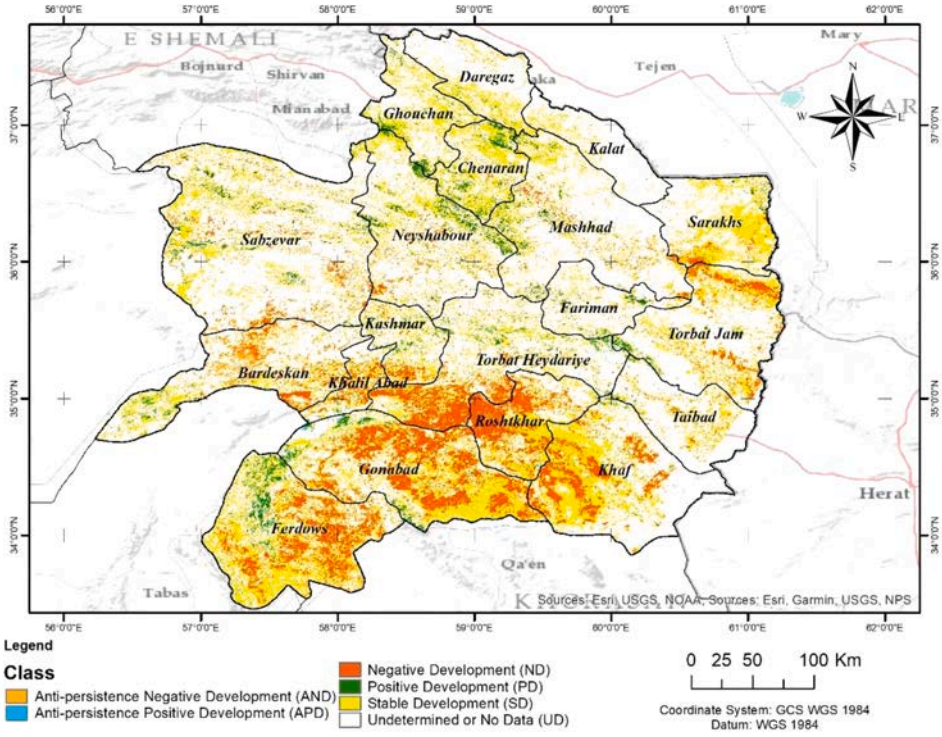

Fig. 5. Expected direction of vegetation development in the future over Khorasan Razavi province. [see text for details]

have been identified as appropriate for establishing environmental restoration activities in order to avoid further degradation of the ecosystems and environment. It should be mentioned that these areas are covered by sparse vegetation (low GSN values) (Fig. 2) and the long-term trends revealed mostly significant decreasing vegetation trends (Fig. 3).

Studying the perspectives for environmental restoration as a function of the de Martonne climatic classes, the results showed that 70.6% of the semi-arid class is likely to have an unspecified trend (Table 5). Due to an increase in dry-farming cultivation during the last decade, and

Table 4
The perspectives for environmental restoration for different LULC types in the Khorasan Razavi province.

	LULC	Area Ratio of Vegetation Development (%)						Restoration Potential Class (see Supplementary Table 2)
		UD	SD	ND	PD	AND	APD	
1	No vegetation cover lands and rocky outcrops	58.5	28.1	7.7	2.5	2.9	0.3	B2
2	Saline lands	43.0	38.4	12.8	2.9	2.5	0.3	A3
3	River beds	64.4	20.6	8.7	1.8	4.1	0.3	C1
4	Shrublands	55.8	23.4	13.1	1.2	6.4	0.2	B2
5	Sand dunes	20.6	27.9	41.3	0.8	9.2	0.3	A4
6	Dense forests	79.4	19.6	0.2	0.2	0.5	0.0	D1
7	Low dense forest	62.6	28.8	4.6	2.1	1.4	0.6	C1
8	Semi-dense forests	70.8	22.5	2.8	0.6	3.1	0.2	C1
9	Reforestation	34.8	26.8	33.0	0.4	4.8	0.2	A4
10	Clay pits	35.3	32.7	25.2	1.1	5.5	0.3	A4
11	Irrigated Farming	62.0	23.6	8.9	1.8	3.3	0.5	C1
12	Dry farming	73.0	18.8	5.9	0.7	1.5	0.1	C1
13	Desert	47.7	34.6	0.6	13.2	0.5	3.4	B3
14	Low density rangelands	52.2	28.6	13.4	2.1	3.5	0.3	B2
15	Dense rangelands	77.4	20.0	0.7	1.6	0.1	0.2	C1
16	Semi-dense rangelands	65.3	24.7	5.5	3.1	1.1	0.4	C1
17	Residential areas	48.6	28.1	11.5	7.8	3.1	0.9	B3
	UD = Undetermined SD = Stable Development ND = Negative Development PD = Positive DevelopmentAND = Anti Persistence Negative Development APD = Anti Persistence Positive Development							

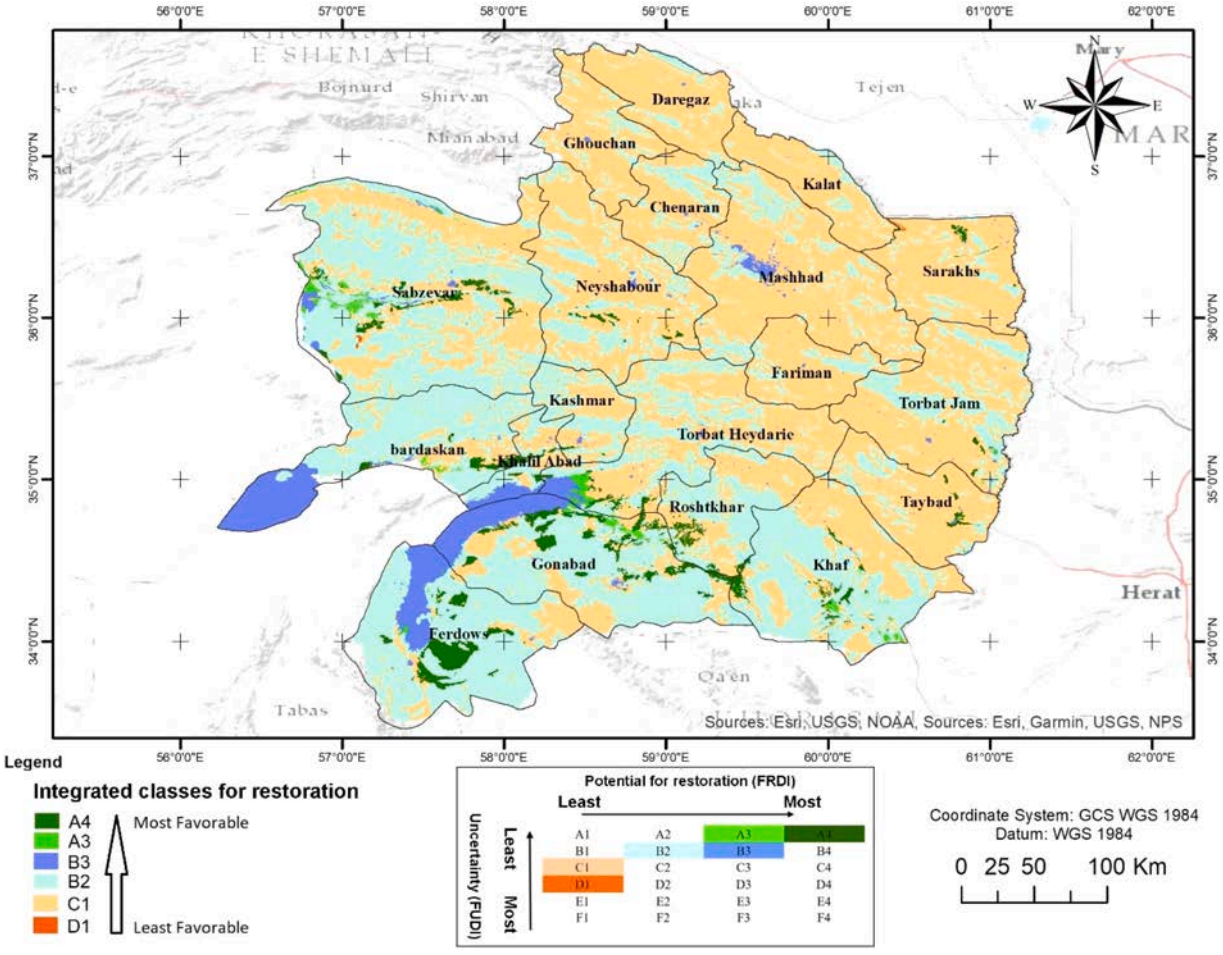

Fig. 6. Map of potential vegetation restoration in Khorasan Razavi province.

considering that these lands are mainly located in arid regions, local people abandoned these lands after cultivation for two - three years. As a consequence, it is predicted that 17.8% and 11.9% of the extra arid and arid areas respectively will have negative development in the future. On the contrary, areas of negative development were much less for semi-humid (0.1%) and Mediterranean (0.04%) climatic classes. Especially for the semi-humid and Mediterranean classes, the effects of precipitation in vegetation development are important, so that at 18.8% and 10.8% of these areas, respectively, the vegetation will be increasing (Table 5). Concerning the restoration potential in the various climatic classes, the extra-arid, semi-humid and Mediterranean types were classified as F2, F3 and F3, respectively (Suppl. Table 4). In these classes,

Table 5
The perspectives for environmental restoration according to the de Martonne classes.

	De Martonne Zone	Area Ratio of Vegetation Development (%)						Restoration Potential Class
		UD	SD	ND	PD	AND	APD	
1	Extra Arid	41.37	31.33	17.83	2.63	6.01	0.83	F2
2	Arid	59.11	24.81	11.89	1.10	2.86	0.23	A2
3	Semi Humid	32.05	48.67	0.10	18.77	0.00	0.41	F3
4	Mediterranean	46.33	42.60	0.04	10.81	0.00	0.22	F3
5	Semi-Arid	70.61	23.30	2.02	3.26	0.38	0.43	A2

despite the relatively favourable conditions for restoration, there is a significant degree of uncertainty that restricts these areas from restoration projects. In contrast, in the arid and semi-arid classes the uncertainty is much lower and, although the FRDI is lower (1.14 – 1.23), these areas – classified as A2 – could be suggested for restoration projects (Suppl. Table 4).

The vegetation trends and perspectives for environmental restoration were also studied for different TNI classes (Table 6). Apart from Class 1, the other classes mostly displayed no specific trend in the vegetation (UD greater than 50%). 50.2% of Class 1 will show a stable behavior in the future, while Class 2 exhibited the most negative development (ND = 15.5%) and this is likely attributed to overlapping with areas of rather low elevation and low slope, which were mostly covered by deserts, sand dunes and rangelands. Class 7 revealed the highest fraction (9.6%) of positive development (Table 6). In terms of restoration potential in TNI classes, the Class 1 was tagged as A4, which indicates favourable conditions for proposing restoration projects, but with high uncertainty (Suppl. Table 5). On the other hand, Classes 3 and 4 were subjected of high uncertainty with very low restoration potential. Classes 2, 7 and 8 were tagged as D3, exhibiting a satisfactory restoration potential, but with relatively high uncertainty. Classes 5 and 6 were grouped as E2 and E3, respectively, indicating some areas with good restoration potential associated with moderate-to-high uncertainty (Table 6; Suppl. Table 5).

3.4. Method validation

The GSN time series was divided into two sub-periods (2004–2009 and 2010–2015) and the pixels that exhibited a statistically-significant trend ($p < 0.05$) were selected for both periods to validate the technique for future trend predictions. Therefore, the vegetation trends were calculated in the first sub-period (2004–2009), and then, the regression slopes were compared to those in the second sub-period (2009–2015) (Table 7). The regression slope of vegetation change in APD class decreased from 46.2% to 5.36% between the two sub-periods, which indicates that the vegetation behavior was as we expected. Furthermore, in AND class the large decreasing trend in the first sub-period (-49.0) disrupts in the second (-3.5), which also meets the definition of the AND (Table 7). Therefore, in areas characterized by a negative trend during 2004–2009, the vegetation continued its decreasing tendency during 2009–2015, but contrary to our predictions, the vegetation stopped increasing in the PD class during the second sub-period (change of the signal from positive to negative). These results show that the Hurst exponent can be used for predicting future changes and is a useful tool for identification of potential areas for establishing environmental restoration projects.

Table 6
The perspectives for environmental restoration according to the TNI classes.

	TNI class	Area Ratio of Vegetation Development (%)						Restoration Potential Class
		UD	SD	ND	PD	AND	APD	
1	0.07–0.2	42.2	50.2	2.8	4.1	0.2	0.4	A4
2	0.2–0.4	51.3	27.3	15.5	1.9	3.5	0.5	D3
3	0.4–0.6	66.3	20.7	9.1	0.7	3.1	0.1	F2
4	0.6–0.8	71.8	21.8	3.1	1.7	1.4	0.2	F1
5	0.8–1	63.3	29.7	1.4	4.4	0.7	0.5	E2
6	1–1.2	56.7	34.1	0.6	7.3	0.4	1.0	E3
7	1.2–1.4	52.6	35.8	0.3	9.6	0.3	1.4	D3
8	1.4–1.97	49.6	39.1	0.9	9.1	0.2	1.0	D3

Table 7
Method validation using the regression slopes in GSN time series for two periods 2004–2009 and 2010–2015.

Predicted Trend(based on 2004–2009 period)	Regression Slope of GSN(2004–09)	Regression Slope of GSN(2009–15)
Anti-Persistent positive trend	46.2	5.35
Anti-Persistent negative trend	−49.01	−3.53
Positive trend	47.92	−13.03
Negative trend	−6.32	−7.02

4. Discussion

The importance of environmental restoration has become a major issue in Iran over the last decade (e.g. Monjezi et al., 2009; Abdollahi et al., 2019; Hosseini et al., 2019a, 2019b; Qaderi Nasab and Rahnama, 2019; Balkanlou et al., 2020), due to anthropogenic impacts and drought conditions under a warmer world scenario that have resulted in vegetation decline, land degradation and increase in dust storms (Rashki et al., 2012; Abbasi et al., 2019; Middleton, 2019). In general, there are two approaches for vegetation restoration: (1) natural restoration and (2) artificial restoration. In natural restoration, the goal is to develop the conditions of the area to improve the current vegetation cover using management actions such as preservation, controlling unauthorized livestock grazing, etc. But in artificial restoration using intervention methods such as seeding, removal of invasive species, fertilization, etc., efforts are made to return the vegetation to its former climax conditions. In this study, the term restoration includes a combination of natural and artificial restoration techniques with more emphasis on natural techniques. Therefore, it is clear that the implementation of restoration projects at the local level requires additional studies and the selection of appropriate species and methods in each region.

Anthropogenic and natural processes may change vegetation cover over time and, in turn, negatively affect ecosystems and biogeochemical cycles (Sun et al., 2009; Mahowald et al., 2017; Kanakidou et al., 2018). Therefore, predicting and – where appropriate – protecting against such deleterious changes in an ecosystem is of vital importance (Pettorelli et al., 2005). Various factors may affect the vegetation dynamics, such as changes in precipitation as well as in topography (Fu et al., 2004, 2009; Sun et al., 2010). Climate change under a warmer world scenario has stronger impacts on arid and semi-arid regions (Middleton, 2018, 2019) and may also negatively affect the inter-relationships between environment, society and human health (Goudie, 2020; Shahsavani et al., 2020). The physical geography of central-south Asia in general, and east Iran in particular, makes these areas more vulnerable to climate change since they have experienced declining precipitation and extensive droughts in recent decades (Mathew et al., 2002; Masoudi et al., 2018; Li et al., 2020; Miri et al., 2021; Rashki et al., 2021). In this respect, the current results showed that 65% of the Khorasan Razavi province area displayed a decreasing trend in vegetation cover, of which 12%

exhibited a statistically significant decrease, mostly observed at the southern and southwestern parts. In contrast, only 2.6% of the province area displayed a statistically-significant increase in GSN, including some parts of the Neyshabur and Chenaran counties, as well as limited areas in the western part of the province (Fig. 3). In addition, some few northern regions of Khorasan Razavi province exhibited an increasing trend in vegetation cover during the last decades, likely attributed to an increase in the cultivated areas. Recurrent drought periods during recent years have severely impacted the hydrological regime resulting in less surface and ground-water availability in Iran (Emadodin et al., 2019). Natural causes, like increase in temperature and decrease in precipitation, may accelerate the vegetation loss and desertification, especially in the mostly arid parts of the southern Khorasan Razavi province (Pashaei et al., 2017). On the other hand, a significant decrease in the desert areas was observed in the Thar Desert, India due to the construction of water canals for transferring water from other regions, thus resulting in increase of greenery and vegetation cover, decrease in soil erosion and dust outflows (Kharol et al., 2013). Such actions may also have beneficial results in preventing land degradation and susceptibility to wind erosion and in improving air quality and human health in Khorasan Razavi province (Najmeddin et al., 2018; Ziyaee et al., 2019; Gholami et al., 2020c). Furthermore, topography has a significant effect on the regional climate by changing the spatial patterns of the local hydrothermal conditions that control vegetation and this was also supported by the current results regarding the changes in vegetation trends for different TNI classes.

As different vegetation types exhibited a contrasting response to climate change, the spatial differentiation of vegetation dynamics has been analyzed for different terrain areas. For a better understanding of the relationship between vegetation and climate change, it is important to investigate the effect of topography and terrain characteristics on vegetation dynamics, along with information on the climatic types. Since a large part of Khorasan Razavi province is located in the arid and semi-arid zones, changes in the temporal and spatial distribution of rainfall would have a drastic effect on the inter-annual variability of NDVI. However, these changes may be interrelated with the growth of perennial vegetation, and for minimizing the effect of temporary vegetation changes, the average vegetation index during the growing season (GSN) was used in this study. Considering the low vegetation cover in northeast Iran, using of NDVI that fails to investigate the soil impacts, would lead to considerable biases in the trend analysis. This is because NDVI is not well-suited to monitoring vegetation changes in dry areas. However, by using the GSN, which covers the entire growth period, such biases would be decreased.

For specific vegetation types in the study area such as sand dunes and clay pits, the vegetation cover has been decreasing markedly, which may have a dramatic effect on the increase in frequency and intensity of dust events (Webb et al., 2016; Middleton, 2018; Duniway et al., 2019; Karimi et al., 2017). Thus, decreasing vegetation cover can increase the surface between wind and soil, and consequently, even weak winds can increase the dust mobilization and emissions (Lim and Chun, 2006; Kim et al., 2017; Parajuli et al., 2019), resulting in degradation of air quality and serious health effects for the local population (Najmeddin et al., 2018).

Studying the perspectives for environmental restoration by analyzing the vegetation trends, highlighted some parts in the Khorasan Razavi province, as the most favourable for implementation of restoration projects. The perceptiveness for restoration was found to decrease for high-elevation areas and steep topographic slopes, considering these terrains rather inappropriate for future restoration projects, since the land surfaces are prone to soil erosion under heavy rains. Implementing restoration projects in certain areas could protect land degradation, and improve the overall quality of the air, soil and water as well as human health and societal indexes.

5. Conclusions

This study analyzed the long-term trends in vegetation cover over Khorasan Razavi province in northeast Iran over the period 2004–2015 using linear regressions of the growing-season NDVI (GSN). MODIS-NDVI time series and GIS applications were synthesized, while the vegetation trends were also examined for different LULC, climatic classes based on the de Martonne climate classification and as a function of the elevation and slope of the area, expressed via the Terrain Niche index (TNI). Furthermore, the vegetation-cover types and the areas that are most favourable for implementing restoration projects were identified, based on combining the Future Restoration Dispersal Index (FRDI) and the Future Uncertainty Dispersal Index (FUDI). The main findings of this study can be summarized as follows:

(1) Generally, vegetation decreased over the period from 2004 to 2015, particularly in southern parts of the province. The topography was found to play an important role in vegetation cover and trends.
(2) Most of the vegetation types displayed no significant trend during the study period. The percentage of pixels showing a decreasing trend in vegetation was greater than pixels with an increasing trend. The Binalood Mountains exhibited mostly increasing trends in vegetation.
(3) The vegetation trends in southern and in some northern parts of the province were found to be mostly stable. The predicted future vegetation showed an unstable trend, especially in the central part of the province. The percentage of vegetation with negative development was greater than vegetation with positive development. Reforestation was found to have the most significant downward trend, which was found to be statistically significant at 95% confidence level ($p = 0.016$). In addition, statistically-significant decreasing trends were also found for the sand dunes, shrublands and clay pits.
(4) In the future, most vegetation-cover decrease is likely to occur in areas affected by human activities, rather than in areas of rough terrain. Some parts in the southwest province were found as the most appropriate for implementation of environmental restoration projects, but with considerable uncertainty. It is suggested that restoration projects should be properly considered to prevent further damage of vegetation and land degradation, since areas that had been restored in the past, exhibited a significant loss of vegetation.

Declaration of Competing Interest

The authors declare that they have no known competing financial interests or personal relationships that could have appeared to influence the work reported in this paper.

Appendix A. Supplementary data

Supplementary data to this article can be found online at https://doi.org/10.1016/j.ecolind.2020.107325.

References

Abbasi, H.R., Opp, C., Groll, M., Rohipour, H., Gohardoust, A., 2019. Assessment of the distribution and activity of dunes in Iran based on mobility indices and ground data. Aeolian Res. 41, 100539. https://doi.org/10.1016/j.aeolia.2019.07.005.

Abdollahi, Z., Kavian, A., Sadeghi, S.H.R., Khosrovyan, A., DelValls, A., 2019. Identifying environmental risk associated with anthropogenic activities in Zanjanrud River, Iran, using an integrated approach. CATENA 183, 104156. https://doi.org/10.1016/j.catena.2019.104156.

Ahmadi, M., Shakiba, A., Roudbari, A.A.D., 2019. Investigating the role of vegetation indices and geographic components on seasonal aerosol optical depth over Iran. J. Earth Space Phys. https://doi.org/10.22059/JESPHYS.2018.260582.1007019.

Arora, V., 2002. Modeling vegetation as a dynamic component in soil-vegetation-atmosphere transfer schemes and hydrological models. Rev. Geophys. 40 (2) https://doi.org/10.1029/2001RG000103.
Azadbar, M., Arzani, H., Azimi, M.S., Mozafarian, V.A., Shad, G.H.A., Saghafi, F., Tavakoli, H., Amir, A.H., Naseri, S., 2011. Rangeland monitoring in the north east of Iran. Iranian J. Range Desert Res. 18, 231–243.
Balkanlou, K.R., Müller, B., Cord, A.F., Panahi, F., Malekian, A., Jafari, M., Egli, L., 2020. Spatiotemporal dynamics of ecosystem services provision in a degraded ecosystem: A systematic assessment in the Lake Urmia basin, Iran. Sci. Total Environ. 716, 137100. https://doi.org/10.1016/j.scitotenv.2020.137100.
Bagherzadeh, A., Mansouri Daneshvar, M.R., 2014. Qualitative Land Suitability Evaluation for Wheat and Barley Crops in Khorasan-Razavi Province, Northeast of Iran. Agric. Res. 3 (2), 155–164. https://doi.org/10.1007/s40003-014-0101-2.
Baude, M., Meyer, B.C., Schindewolf, M., 2019. Land use change in an agricultural landscape causing degradation of soil based ecosystem services. Sci. Total Environ. 659, 1526–1536. https://doi.org/10.1016/j.scitotenv.2018.12.455.
Boiral, O., Heras-Saizarbitoria, I., Brotherton, M.-C., 2019. Nature connectedness and environmental management in natural resources companies: An exploratory study. J. Cleaner Prod. 206, 227–237. https://doi.org/10.1016/j.jclepro.2018.09.174.
Boroughani, M., Pourhashemi, S., Hashemi, H., Salehi, M., Amirahmadi, A., Asadi, M.A. Z., Berndtsson, R., 2020. Application of remote sensing techniques and machine learning algorithms in dust source detection and dust source susceptibility mapping. Ecol. Inf. 56, 101059. https://doi.org/10.1016/j.ecoinf.2020.101059.
Braswell, B.H., Schimel, D.S., Linder, E., Moore, B., 1997. The response of global terrestrial ecosystems to interannual temperature variability. Science 278 (5339), 870–873. https://doi.org/10.1126/science.278.5339.870.
Burnett, K.M., Ticktin, T., Bremer, L.L., Quazi, S.A., Geslani, C., Wada, C.A., Kurashima, N., Mandle, L., Pascua, P., Depraetere, T., Wolkis, D., Edmonds, M., Giambelluca, T., Falinski, K., Winter, K.B., 2019. Restoring to the future: Environmental, cultural, and management trade-offs in historical versus hybrid restoration of a highly modified ecosystem. Conservat. Lett. 12 (1), e12606. https://doi.org/10.1111/conl.12606.
Bunting, E.L., Fullman, T., Kiker, G., Southworth, J., 2016. Utilization of the SAVANNA model to analyze future patterns of vegetation cover in Kruger National Park under changing climate. Ecol. Model. 342, 147–160. https://doi.org/10.1016/j.ecolmodel.2016.09.012.
de Martonne, E., 1942. Nouvelle carte mondiale de l'indice d'aridité (Carte hors texte). Annales de Géographie, 51(288), 241–250. JSTOR. https://doi.org/10.3406/geo.1942.12050.
Duniway, M.C., Pfennigwerth, A.A., Fick, S.E., Nauman, T.W., Belnap, J., Barger, N.N., 2019. Wind erosion and dust from US drylands: a review of causes, consequences, and solutions in a changing world. Ecosphere 10 (3), e02650. https://doi.org/10.1002/ecs2.2650.
Emadodin, I., Reinsch, T., Taube, F., 2019. Drought and Desertification in Iran. Hydrology 6(3), 66. Doi: 10.3390/hydrology6030066.
Fabricante, I., Oesterheld, M., Paruelo, J.M., 2009. Annual and seasonal variation of NDVI explained by current and previous precipitation across Northern Patagonia. J. Arid Environ. 73 (8), 745–753. https://doi.org/10.1016/j.jaridenv.2009.02.006.
Fang, J., Piao, S., He, J., Ma, W., 2004. Increasing terrestrial vegetation activity in China, 1982–1999. Sci. China Ser. C.-Life Sci. 47 (3), 229–240. https://doi.org/10.1007/BF03182768.
Fensholt, R., Rasmussen, K., Nielsen, T.T., Mbow, C., 2009. Evaluation of earth observation based long term vegetation trends — Intercomparing NDVI time series trend analysis consistency of Sahel from AVHRR GIMMS, Terra MODIS and SPOT VGT data. Remote Sens. Environ. 113 (9), 1886–1898. https://doi.org/10.1016/j.rse.2009.04.004.
Fu, B.-J., Wang, Y.-F., Lu, Y.-H., He, C.-S., Chen, L.-D., & Song, C.-J., 2009. The effects of land-use combinations on soil erosion: a case study in the Loess Plateau of China. Progr. Phys. Geogr., 33(6), 793–804. Doi: 10.1177%2F0309133309350264.
Fu, B.J., Liu, S.L., Ma, K.M., Zhu, Y.G., 2004. Relationships between soil characteristics, topography and plant diversity in a heterogeneous deciduous broad-leaved forest near Beijing, China. Plant Soil 261 (1/2), 47–54. https://doi.org/10.1023/B:PLSO.0000035567.97093.48.
Fu, B., Li, S., Yu, X., Yang, P., Yu, G., Feng, R., Zhuang, X., 2010. Chinese ecosystem research network: Progress and perspectives. Ecol. Complexity 7 (2), 225–233. https://doi.org/10.1016/j.ecocom.2010.02.007.
Gilbey, B., Davies, J., Metternicht, G., Magero, C., 2019. Taking Land Degradation Neutrality from concept to practice: Early reflections on LDN target setting and planning. Environ. Sci. Policy 100, 230–237. https://doi.org/10.1016/j.envsci.2019.04.007.
Gholami, H., Mohammadifar, A., Bui, D.T., Collins, A.L., 2020a. Mapping wind erosion hazard with regression-based machine learning algorithms. Sci. Rep. 10 (1) https://doi.org/10.1038/s41598-020-77567-0.
Gholami, H., Mohamadifar, A., Sorooshian, A., Jansen, J.D., 2020b. Machine-learning algorithms for predicting land susceptibility to dust emissions: The case of the Jazmurian Basin, Iran. Atmos. Pollut. Res. 11 (8), 1303–1315. https://doi.org/10.1016/j.apr.2020.05.009.
Gholami, H., Mohamadifar, A., Collins, A.L., 2020c. Spatial mapping of the provenance of storm dust: Application of data mining and ensemble modelling. Atmos. Res. 233, 104716. https://doi.org/10.1016/j.atmosres.2019.104716.
Goudie, A.S., 2020. Dust Storms and Human Health. In book: Extreme Weather Events and Human Health, doi: 10.1007/978-3-030-23773-8_2.
Hague, B., 2016. The use of remote sensing to map and monitor coastal dune vegetation change at Southampton, Ontario, Canada. http://hdl.handle.net/10464/9290.
Hanson, D.A., Britney, E.M., Earle, C.J., Stewart, T.G., 2013. Adapting Habitat Equivalency Analysis (HEA) to assess environmental loss and compensatory restoration following severe forest fires. For. Ecol. Manage. 294, 166–177. https://doi.org/10.1016/j.foreco.2012.12.032.
HOLBEN, B.N., 1986. Characteristics of maximum-value composite images from temporal AVHRR data. Int. J. Remote Sens. 7 (11), 1417–1434. https://doi.org/10.1080/01431168608948945.
Hosseini, S., Ivanov, D., Dolgui, A., 2019a. Review of quantitative methods for supply chain resilience analysis. Transport. Res. Part E: Logist. Transport. Rev. 125, 285–307. https://doi.org/10.1016/j.tre.2019.03.001.
Hosseini, S.M., Parizi, E., Ataie-Ashtiani, B., Simmons, C.T., 2019b. Assessment of sustainable groundwater resources management using integrated environmental index: Case studies across Iran. Sci. Total Environ. 676, 792–810. https://doi.org/10.1016/j.scitotenv.2019.04.257.
Hu, C., Fu, B., Liu, G., Jin, T., Guo, L., 2010. Vegetation patterns influence on soil microbial biomass and functional diversity in a hilly area of the Loess Plateau, China. J. Soils Sediments 10 (6), 1082–1091. https://doi.org/10.1007/s11368-010-0209-3.
Huang, X., Yuan, H., Yu, F., Li, X., Liang, Q., Yao, P., Shao, H., 2013. Spatial–temporal succession of the vegetation in Xishuangbanna, China during 1976–2010. Ecol. Eng. 70, 255–262. https://doi.org/10.1016/j.ecoleng.2014.05.022.
Hubbard, S., Hornsby, K.S., 2011. Modeling Alternative Sequences of Events in Dynamic Geographic Domains. Transactions GIS. Doi: 10.1111/j.1467-9671.2011.01279.x.
Hurst, H.E., 1951. Long-term storage capacity of reservoirs. Trans. Amer. Soc. Civil Eng. 116, 770–799. https://doi.org/10.1080/02626665609493644.
Jiang, W., Yuan, L., Wang, W., Cao, R., Zhang, Y., Shen, W., 2015. Spatio-temporal analysis of vegetation variation in the Yellow River Basin. Ecol. Ind. 51, 117–126. https://doi.org/10.1016/j.ecolind.2014.07.031.
Kanakidou, M., Myriokefalitakis, S., Tsigaridis, K., 2018. Aerosols in atmospheric chemistry and biogeochemical cycles of nutrients. Environ. Res. Lett. 13 (6), 063004. https://doi.org/10.1088/1748-9326/aabcdb.
Karimi, A., Haghnia, G.H., Safari, T., Hadadian, H., 2017. Lithogenic and anthropogenic pollution assessment of Ni, Zn and Pb in surface soils of Mashhad plain, northeastern Iran. CATENA 157, 151–162. https://doi.org/10.1016/j.catena.2017.05.019.
Kelly, M., Tuxen, K.A., Stralberg, D., 2011. Mapping changes to vegetation pattern in a restoring wetland: Finding pattern metrics that are consistent across spatial scale and time. Ecol. Ind. 11 (2), 263–273. https://doi.org/10.1016/j.ecolind.2010.05.003.
Kelly, T.J., Lawson, I.T., Roucoux, K.H., Baker, T.R., Honorio Coronado, E.N., 2020. Patterns and drivers of development in a west Amazonian peatland during the late Holocene. Quat. Sci. Rev. 230, 106168. https://doi.org/10.1016/j.quascirev.2020.106168.
Kharol, S.K., Kaskaoutis, D.G., Badarinath, K.V.S., Sharma, A.R., Singh, R.P., 2013. Influence of land use/land cover (LULC) changes on atmospheric dynamics over the arid region of Rajasthan state, India. J. Arid Environ. 88, 90–101. https://doi.org/10.1016/j.jaridenv.2012.09.006.
Khusfi, Z.E., Khosroshahi, M., Roustaei, F., Mirakbari, M., 2020. Spatial and seasonal variations of sand-dust events and their relation to atmospheric conditions and vegetation cover in semi-arid regions of central Iran. Geoderma 365, 114225. https://doi.org/10.1016/j.geoderma.2020.114225.
Kiani-Harchegani, M., Sadeghi, S.H., 2020. Practicing land degradation neutrality (LDN) approach in the Shazand Watershed, Iran. Sci. Total Environ. 698, 134319. https://doi.org/10.1016/j.scitotenv.2019.134319.
Kim, D., Chin, M., Remer, L.A., Diehl, T., Bian, H., Yu, H., Brown, M.E., Stockwell, W.R., 2017. Role of surface wind and vegetation cover in multi-decadal variations of dust emission in the Sahara and Sahel. Atmos. Environ. 148, 282–296. https://doi.org/10.1016/j.atmosenv.2016.10.051.
Li, Y., Gholami, H., Song, Y., Fathabadi, A., Malakooti, H., Collins, A.L., 2020. Source fingerprinting loess deposits in Central Asia using elemental geochemistry with Bayesian and GLUE models. CATENA 194, 104808. https://doi.org/10.1016/j.catena.2020.104808.
Lei, S., Zhang, F., Yan, Y., Liu, X., 2016. Spatial-temporal changes and future trends of vegetation cover in upper reaches of Heihe river. Bull. Soil Water Conserv. 36, 159–164. https://doi.org/10.3390/su7010366.
Lim, Ju-Yeon, Chun, Youngsin, 2006. The characteristics of Asian dust events in Northeast Asia during the springtime from 1993 to 2004. Global Planet. Change 52 (1-4), 231–247. https://doi.org/10.1016/j.gloplacha.2006.02.010.
Lotfalinezhad, Hamze, Maleki, Ali, 2020. TTA, a new approach to estimate Hurst exponent with less estimation error and computational time. Physica A Statist. Mechan. Appl. 553, 124093. https://doi.org/10.1016/j.physa:2019.124093.
Lu, Qing, Zhao, Dongsheng, Wu, Shaohong, Dai, Erfu, Gao, Jiangbo, 2019. Using the NDVI to analyze trends and stability of grassland vegetation cover in Inner Mongolia. Theor. Appl. Climatol. 135 (3-4), 1629–1640. https://doi.org/10.1007/s00704-018-2614-2.
Mahowald, Natalie M., Scanza, Rachel, Brahney, Janice, Goodale, Christine L., Hess, Peter G., Moore, J. Keith, Neff, Jason, 2017. Aerosol Deposition Impacts on Land and Ocean Carbon Cycles. Curr. Clim. Change Rep. 3 (1), 16–31. https://doi.org/10.1007/s40641-017-0056-z.
Mandelbrot, Benoit B., Wallis, James R., 1969. Robustness of the rescaled range R/S in the measurement of noncyclic long run statistical dependence. Water Resour. Res. 5 (5), 967–988. https://doi.org/10.1029/WR005i005p00967.
Masoudi, M., Yousefi, M., & Behbahani, N., 2018. Hazard Assessment of Climate Changes in South Khorasan Province, Iran. EQA – Int. J. Environ. Quality; Vol 29 (2018). Doi: 10.6092/Issn.2281-4485/7910.
Mathew, B., Cullen, H., Lyon, B., 2002. Drought in central and Southwest Asia: La Nina, the warm pool, and Indian Ocean precipitation. J. Climate 15, 697–700. https://doi.org/10.1175/1520-0442(2002)015%3C0697:DICASA%3E2.0.CO;2.
Middleton, N., 2018. Rangeland management and climate hazards in drylands: dust storms, desertification and the overgrazing debate. Nat. Hazards 92 (S1), 57–70. https://doi.org/10.1007/s11069-016-2592-6.

Middleton, N.J., 2019. Variability and Trends in Dust Storm Frequency on Decadal Timescales: Climatic Drivers and Human Impacts. Geosciences 9, 261. https://doi.org/10.3390/geosciences9060261.

Miri, A., Maleki, S., Middleton, N., 2021. An investigation into climatic and terrestrial drivers of dust storms in the Sistan region of Iran in the early twenty-first century. Sci. Total Environ. 757, 143952 https://doi.org/10.1016/j.scitotenv.2020.143952.

Monjezi, M., Shahriar, K., Dehghani, H., Samimi Namin, F., 2009. Environmental impact assessment of open pit mining in Iran. Environ. *Geology* 58, 205–216. https://doi.org/10.1007/s00254-008-1509-4.

Mosavi Baygi, M., Ashraf, B., 2011. Study of leading to drought of autumn and winter synoptic patterns in Khorasan Razavi Province. J. Soil Water Conserv., 18(4), 184-621 167. (in Persian). magiran.com/p1012078.

Myneni, R.B., Keeling, C.D., Tucker, C.J., Asrar, G., Nemani, R.R., 1997. Increased plant growth in the northern high latitudes from 1981 to 1991. Nature 386, 698. https://doi.org/10.1038/386698a0.

Najmeddin, A., Moore, F., Keshavarzi, B., Sadegh, Z., 2018. Pollution, source apportionment and health risk of potentially toxic elements (PTEs) and polycyclic aromatic hydrocarbons (PAHs) in urban street dust of Mashhad, the second largest city of Iran. J. Geochem. Exploration 190, 154–169. https://doi.org/10.1016/j.gexplo.2018.03.004.

Nemani, R.R., 2003. Climate-Driven Increases in Global Terrestrial Net Primary Production from 1982 to 1999. Science 300 (5625), 1560–1563. https://doi.org/10.1126/science.1082750.

Peng, J., Liu, Z., Liu, Y., Wu, J., Han, Y., 2012. Trend analysis of vegetation dynamics in Qinghai-Tibet Plateau using Hurst Exponent. Ecol. Ind. 14 (1), 28–39. https://doi.org/10.1016/j.ecolind.2011.08.011.

Parajuli, S.P., Stenchikov, G.L., Ukhov, A., Kim, H., 2019. Dust emission modeling using a new high-resolution dust source function in WRF-Chem with implications for air quality. J. Geophys. Res. Atmospheres 124 (17–18), 10109–10133.

Pashaei, M., Rashki, A., Sepehr, A., 2017. An Integrated Desertification Vulnerability Index for Khorasan-Razavi, Iran. Natural Res. Conservation 5 (3), 44–55. https://doi.org/10.13189/nrc.2017.050302.

Pettorelli, N., Vik, J.O., Mysterud, A., Gaillard, J.-M., Tucker, C.J., Stenseth, N.C., 2005. Using the satellite-derived NDVI to assess ecological responses to environmental change. Trends Ecol. Evol. 20 (9), 503–510. https://doi.org/10.1016/j.tree.2005.05.011.

Piao, S., Fang, J., 2003. Seasonal Changes in Vegetation Activity in Response to Climate Changes in China between1982and1999. Acta Geogr. Sin. 1.

Poorhashemi, S., Ahmadi, A.A., Zangane, M.A., Salehi, M., 2019. Identification and Characterization of Dust Source in Khorasan Razavi Province. Geogr. Res. 34 (1), 1–10. https://doi.org/10.29252/geores.34.1.1.

Rahimi, J., Ebrahimpour, M., Khalili, A., 2013. Spatial changes of Extended De Martonne climatic zones affected by climate change in Iran. Theor. Appl. Climatol. 112 (3), 409–418. https://doi.org/10.1007/s00704-012-0741-8.

Rashki, A., Kaskaoutis, D.G., Rautenbach, C.J.deW., Eriksson, P.G., Qiang, M., Gupta, P., 2012. Dust storms and their horizontal dust loading in the Sistan region, Iran. Aeol. Res. 5, 51–62. https://doi.org/10.1016/j.aeolia.2011.12.001.

Rashki, A., Kaskaoutis, D.G., Sepehr, A., 2018. Statistical evaluation of the dust events at selected stations in southwest Asia: from the Caspian Sea to the Arabian Sea. Catena 165, 590–603. https://doi.org/10.1016/j.catena.2018.03.011.

Rashki, A., Middleton, N.J., Goudie, A.S., 2021. Dust storms in Iran – Distribution, causes, frequencies and impacts. Aeol. Res. 48, 100655 https://doi.org/10.1016/j.aeolia.2020.100655.

Sánchez Granero, M.A., Trinidad Segovia, J.E., García Pérez, J., 2008. Some comments on Hurst exponent and the long memory processes on capital markets. Physica A: Statist. Mechan. Appl. 387, 5543–5551. https://doi.org/10.1016/j.physa.2008.05.053.

Shahsavani, A., Tobías, A., Querol, X., Stafoggia, M., Abdolshahnejad, M., Mayvaneh, F., Guo, Y., Hadei, M., Hashemi, S.S., Khosravi, A., Namvar, Z., Yarahmadi, M., Emam, B., 2020. Short-term effects of particulate matter during desert and non-desert dust days on mortality in Iran. Environ. Intern. 134, 105299 https://doi.org/10.1016/j.envint.2019.105299.

Sharifikia, M., 2013. Environmental challenges and drought hazard assessment of Hamoun Desert Lake in Sistan region, Iran, based on the time series of satellite imagery. Nat. Hazards 65, 201–217. https://doi.org/10.1007/s11069-012-0353-8.

Shataee, S., & Abdi, O., 2007. Land Cover Mapping in Mountainous Lands of Zagros Using ETM+ Data (Case Study: Sorkhab Watershed, Lorestan Province). Agric. Sci. Natur. Resour, 14.

Shiravi, M., Sepehr, A., 2017. Fuzzy Based Detection of Desertification-Prone Areas: A Case Study in Khorasan-Razavi Province. Iran. Geography.

Shuang-cheng, L.I., Zhi-qiang, Z., Yang, G., Yang-lin, W., 2008. Determining the predictability and the spatial pattern of urban vegetation using recurrence quantification analysis: a case study of Shenzhen City. Geograp. Res. 27 (6), 1243–1252. https://doi.org/10.1140/epjst/e2008-00839-y.

Soltani, Gholipoor, M., 2006. Teleconnections Between El Nino/Southern Oscillation and Rainfall and Temperature in Iran. Int. J. Agricul. Res. 1, 603–608. https://doi.org/10.3923/ijar.2006.603.608.

Sun, Zh., Opp, Ch., Run, W., 2009. Vegetation response to ecological water diversion in the lower Tarim River, Xinjiang, China. Basic Appl. Dryland Res. 3, 1–16.

Sun, Z., Chang, N.-B. & Opp, Ch. (2010): Using SPOT-VGT NDVI as a successive ecological indicator for understanding the environmental implications in the Tarim River Basin, China. Journal of Applied Remote Sensing 4: 1-19.Sun, Y.-L., Shan, M., Pei, X.-R., Zhang, X.-K., & Yang, Y.-L., 2020. Assessment of the impacts of climate change and human activities on vegetation cover change in the Haihe River basin, China. Phys. Chem. Earth, Parts A/B/C, 115, 102834. Doi: 10.1016/j.pce.2019.102834.

Suzuki, R., Masuda, K., Dye, G., 2007. Interannual covariability between actual evapotranspiration and PAL and GIMMS NDVIs of northern Asia. Remote Sens. Environ. 106 (3), 387–398. https://doi.org/10.1016/j.rse.2006.10.016.

Svoray, T., Perevolotsky, A., Atkinson, P.M., 2013. Ecological sustainability in rangelands: the contribution of remote sensing. Int. J. Remote Sens. 34 (17), 6216–6242. https://doi.org/10.1080/01431161.2013.793867.

Tong, S., Zhang, J., Bao, Y., Lai, Q., Lian, X., Li, N., Bao, Y., 2018. Analyzing vegetation dynamic trend on the Mongolian Plateau based on the Hurst exponent and influencing factors from 1982–2013. J. Geog. Sci. 28 (5), 595–610. https://doi.org/10.1007/s11442-018-1493-x.

Tong, X., Wang, K., Brandt, M., Yue, Y., Liao, C., Fensholt, R., 2016. Assessing future vegetation trends and restoration prospects in the Karst regions of Southwest China. Remote Sensing 8 (5), 1–17. https://doi.org/10.3390/rs8050357.

Tucker, C.J., Slayback, D.A., Pinzon, J.E., Los, S.O., Myneni, R.B., Taylor, M.G., 2001. Higher northern latitude normalized difference vegetation index and growing season trends from 1982 to 1999. Int. J. Biometeorol. 45 (4), 184–190. https://doi.org/10.1007/s00484-001-0109-8.

Vaisi, V., Heydarnezhad, S., & Fordoei, R., 2016. Analysis of Vegetation Changes in Iran Using Modis Satellite Images (In persian). The First International Conference and the Second National Confernce on Agriculture, Environment and Food Security. https://www.civilica.com/Paper-AEFSJ02-AEFSJ02_181.html.

Vadrevu, K.P., Lasko, K., Giglio, L., Justice, C., 2015. Vegetation fires, absorbing aerosols and smoke plume characteristics in diverse biomass burning regions of Asia. Environ. Res. Lett. 10, 105003 https://doi.org/10.1088/1748-9326/10/10/105003.

Wang, Y., Wang, Z., Li, R., Meng, X., Ju, X., Zhao, Y., Sha, Z., 2018. Comparison of Modeling Grassland Degradation with and without Considering Localized Spatial Associations in Vegetation Changing Patterns. Sustainability 10. https://doi.org/10.3390/su10020316.

Webb, N.P., Herrick, J.E., Van Zee, J.W., Courtright, E.M., Hugenholtz, C.H., Zobeck, T. M., Wagner, L., 2016. The National Wind Erosion Research Network: Building a standardized long-term data resource for aeolian research, modeling and land management. Aeolian Res. 22, 23–36. https://doi.org/10.1016/j.aeolia.2016.05.005.

Wu, Z., Wu, J., Liu, J., He, B., Lei, T., Wang, Q., 2013. Increasing terrestrial vegetation activity of ecological restoration program in the Beijing-Tianjin Sand Source Region of China. Ecol. Eng. 52, 37–50. https://doi.org/10.1016/j.ecoleng.2012.12.040.

Xiao, J., Bai, X., Zhou, D., Qian, Q., Zeng, C., Chen, F., 2018. Spatial-temporal Evolution of Vegetation Coverage and Analysis of it's Future Trends in Wujiang River Basin. IOP Conference Series: Earth Environ. Sci. 108, 42066. https://doi.org/10.1088/1755-1315/108/4/042066.

Yi, Y., Kimball, J.S., Reichle, R.H., 2014. Spring hydrology determines summer net carbon uptake in northern ecosystems. Environ. Res. Lett. 9, 064003 https://doi.org/10.1088/1748-9326%2F9%2F6%2F064003.

Yue-cong, Z., Zhi-qiang, Z., Shuang-cheng, L.I., Xian-feng, M., 2008. Indicating variation of surface vegetation cover using SPOT NDVI in the northern part of North China. Geograph. Res. 27 (4), 745–755. https://doi.org/10.11821/yj2008040003.

Zhang, G., Dong, J., Xiao, X., Hu, Z., Sheldon, S., 2012. Effectiveness of ecological restoration projects in Horqin Sandy Land, China based on SPOT-VGT NDVI data. Ecol. Eng. 38 (1), 20–29. https://doi.org/10.1016/j.ecoleng.2011.09.005.

Ziyaee, A., Hirmas, D.R., Karimi, A., Kehl, M., Macpherson, G.L., Lakzian, A., Roshanizarmehri, M., 2019. Geogenic and anthropogenic sources of potentially toxic elements in airborne dust in northeastern Iran. Aeol. Res. 41, 100540 https://doi.org/10.1016/j.aeolia.2019.100540.

Ziyaee, A., Karimi, A., Hirmas, D.R., Kehl, M., Lakzian, A., Khademi, H., Mechem, D.B., 2018. Spatial and temporal variations of airborne dust fallout in Khorasan Razavi Province, Northeastern Iran. Geoderma 326, 42–55. https://doi.org/10.1016/j.geoderma.2018.04.010.

Zoljoodi, M., Didevarasl, A., 2013. Evaluation of spatial-temporal variability of drought events in Iran using palmer drought severity index and its principal factors (through 1951–2005). Atmos. *Clim. Sci.* 3, 193–207. https://doi.org/10.4236/acs.2013.32021.